# Translating compositional Earth models into realistic computational models with consideration to the complexity of geological constraints

Andrew Long, Director,



#### Scheme

Compositional and rheological models Established modelling methods

Seeing primary order structure

Handling time: the fourth dimension

Some examples: kimberlites and earthquakes

Conclusions

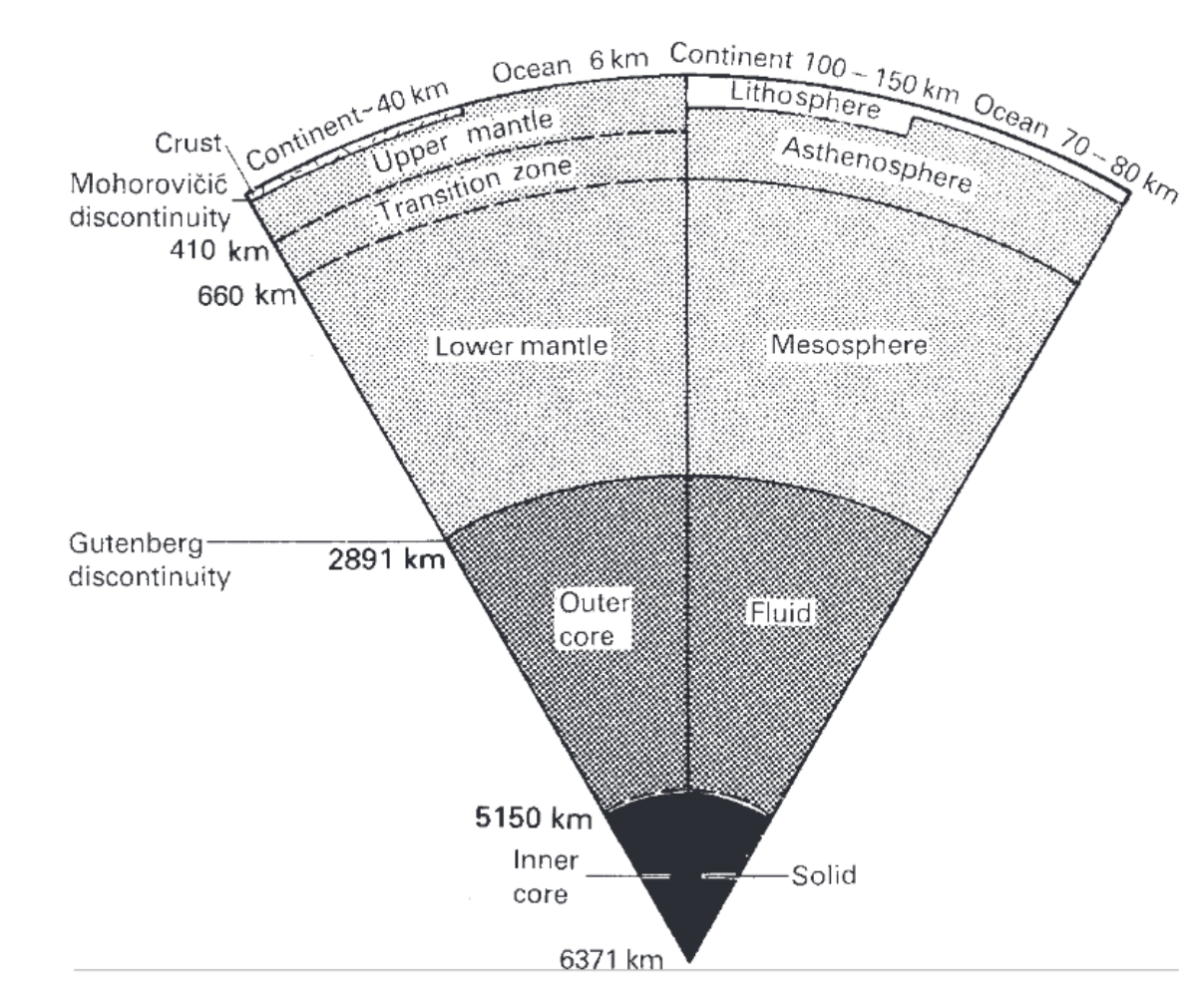


#### Compositional and rheological Earth models

Compositional layering

Rheological layering

Density, Seismic Velocity



Brittle failure, ductile flow Strength, Mpa Stress, Strain Property definition of the lithosphere? Temperature

Source: Global tectonics Kearey et al, 1990



**Figure 2.39** Comparison of the compositional and rheological layering of the Earth.

# Established modelling methods

Analogue modelling (plasticine, sand)

#### Digital modelling of geophysical data

1D, 2D parametric layers with limited anisotropy and 3D cell/mesh based anisotropy. Statistical methods. Spherical harmonics (Stokes coefficients)

Property discretization, assumptions, constraints, minimising measured and calculated error misfit, and error fitting trade offs

Definition of "geology"

#### Analogue example Adda et al 2017

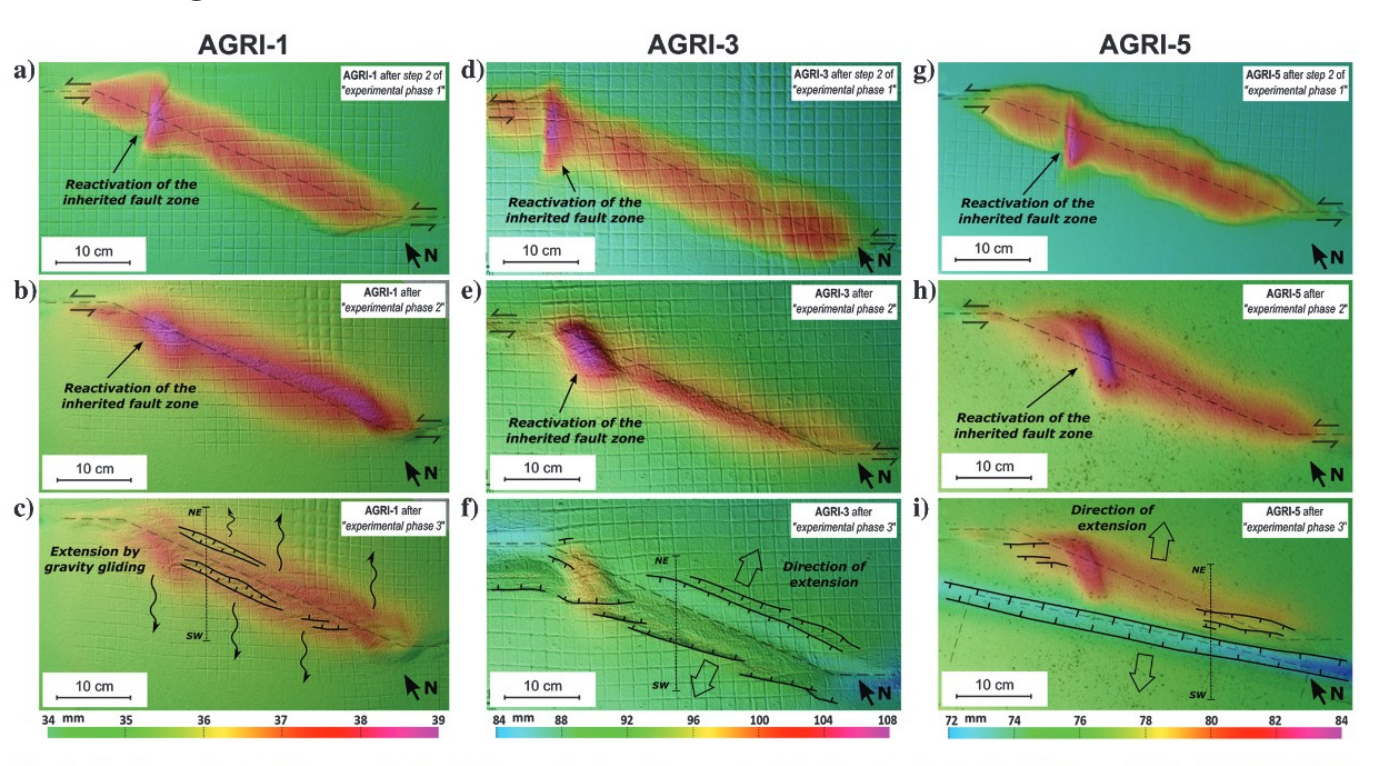
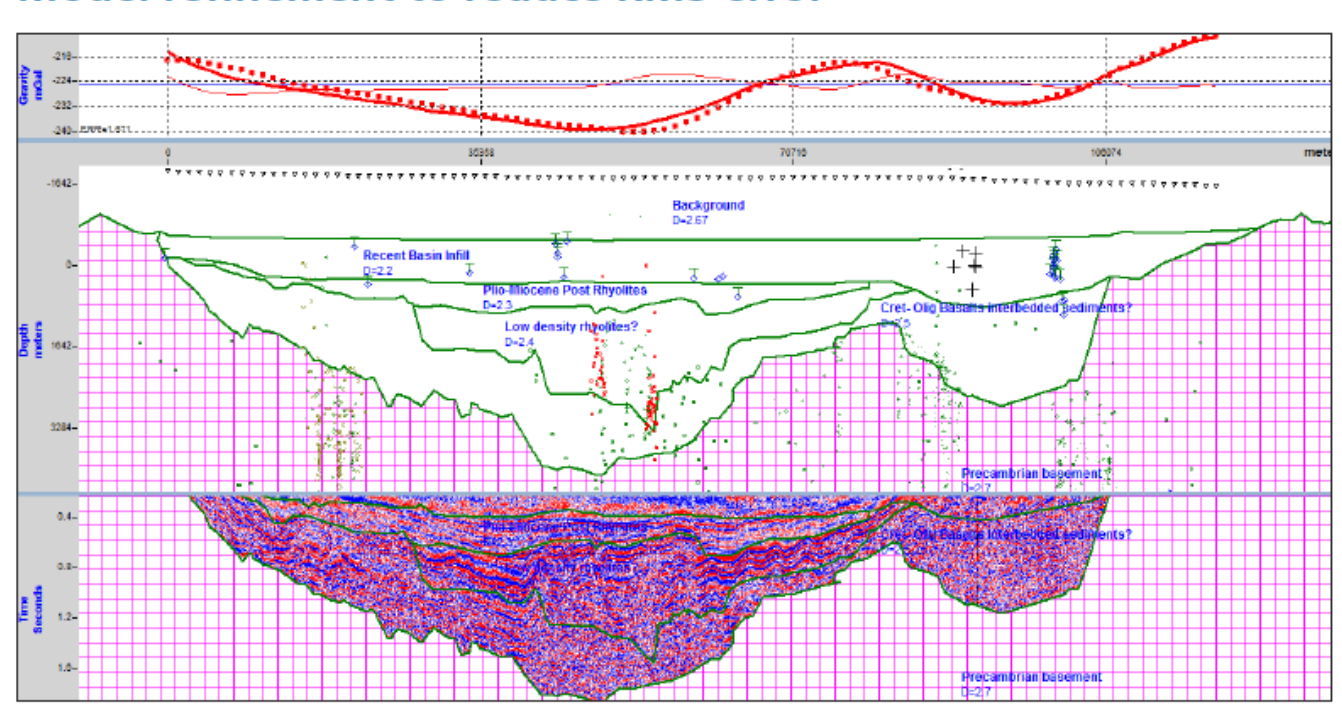


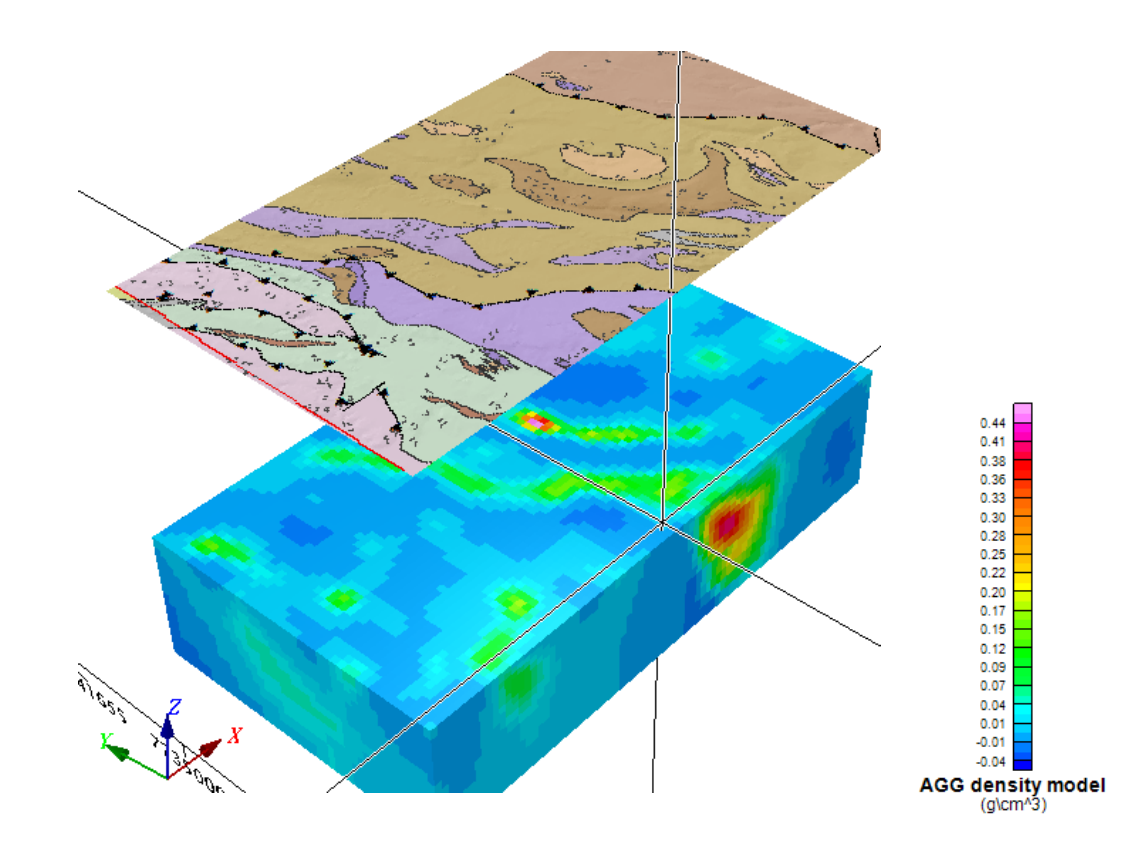
**Figure 4.** Comparison of top overhead pictures with draped corresponding topography (colors) for model (a-c) AGRI-1, (d-f) AGRI-3, and (g-i) AGRI-5, after step 2 of experimental phase 1 (a, d, g), after experimental phase 2 (b, e, h), and after experimental phase 3 (c, f, i). The main formed structures have been highlighted, and the locations of cross sections shown in Figure 5 are indicated with dashed lines.



### 2D Profile and 3D modelling

#### Model refinement to reduce RMS error





Traditional profile modelling Extract from Long et al, 2011

Regularized smooth cell 3D inversion Extract from Long et al, 2013



# Primary order structure – "tectonics"

Long wavelength structure can only be captured by geophysical measurements over large distances (1000s kms), and is dependent on coverage and sampling resolution

Satellite gravity and magnetics

Seismicity - Seismic tomography

Other regional survey methods (2D profiles, e.g. SAMTEX)



#### Station coverage

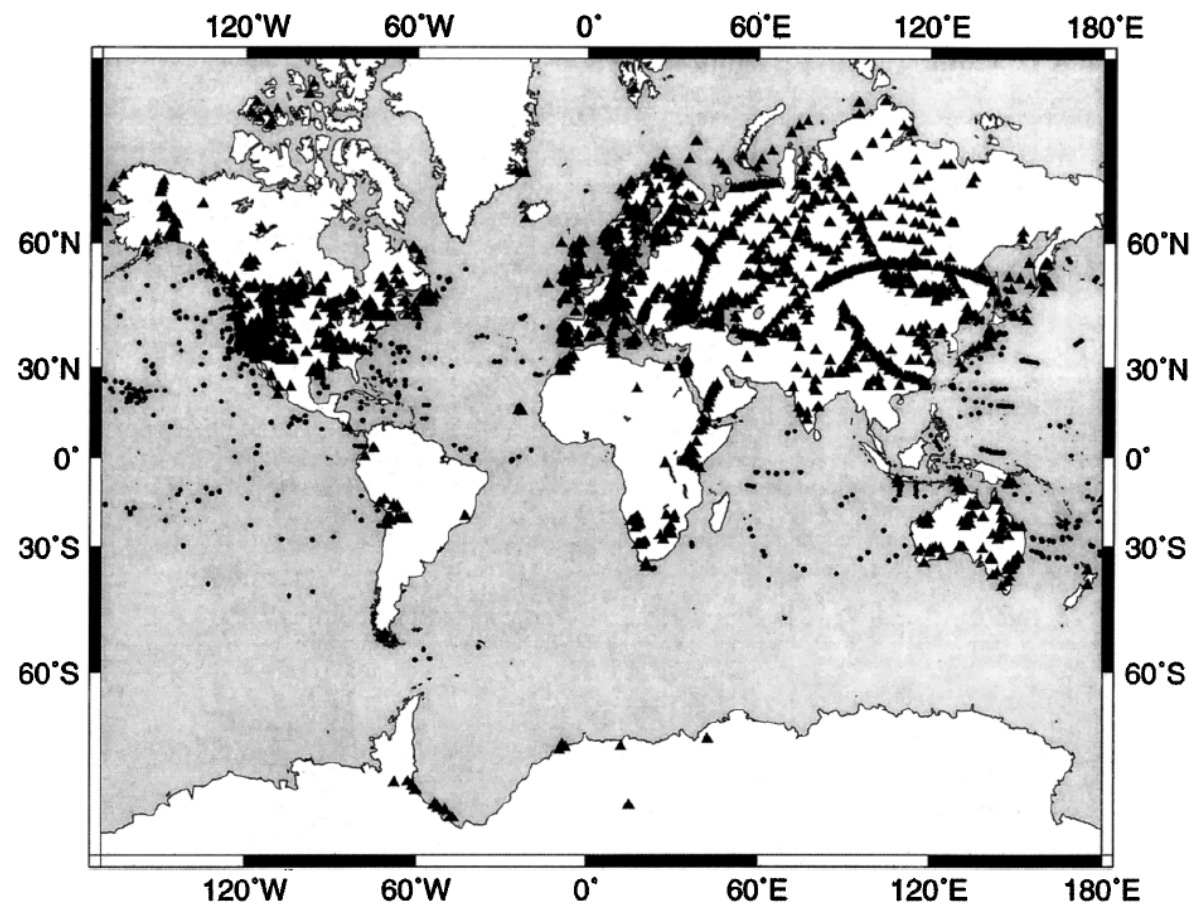


Figure 1. Location of seismic refraction profiles used in this study. Triangles correspond to locations within continents and on margins where a velocity-depth function has been extracted from a published crustal interpretation. These locations are generally at the midpoint between shot points along each profile. These data provide details on the compressional wave seismic velocity structure and, in about 10% of the cases, also the shear wave structure of the crust in a wide range of tectonic settings (Figure 2). Sources are cited by Christensen and Mooney [1995]. Solid circles are locations of oceanic refraction profiles [Christensen, 1982]. A standard crustal model is used for normal oceanic crust, and appropriate models are used for oceanic plateaus and other features (Figure 2 and text). Data selection and interpretation uncertainties are discussed in the text.

CRUST 5.1: A global crustal model at 5 × 5 degrees

#### Mooney et al, 1998

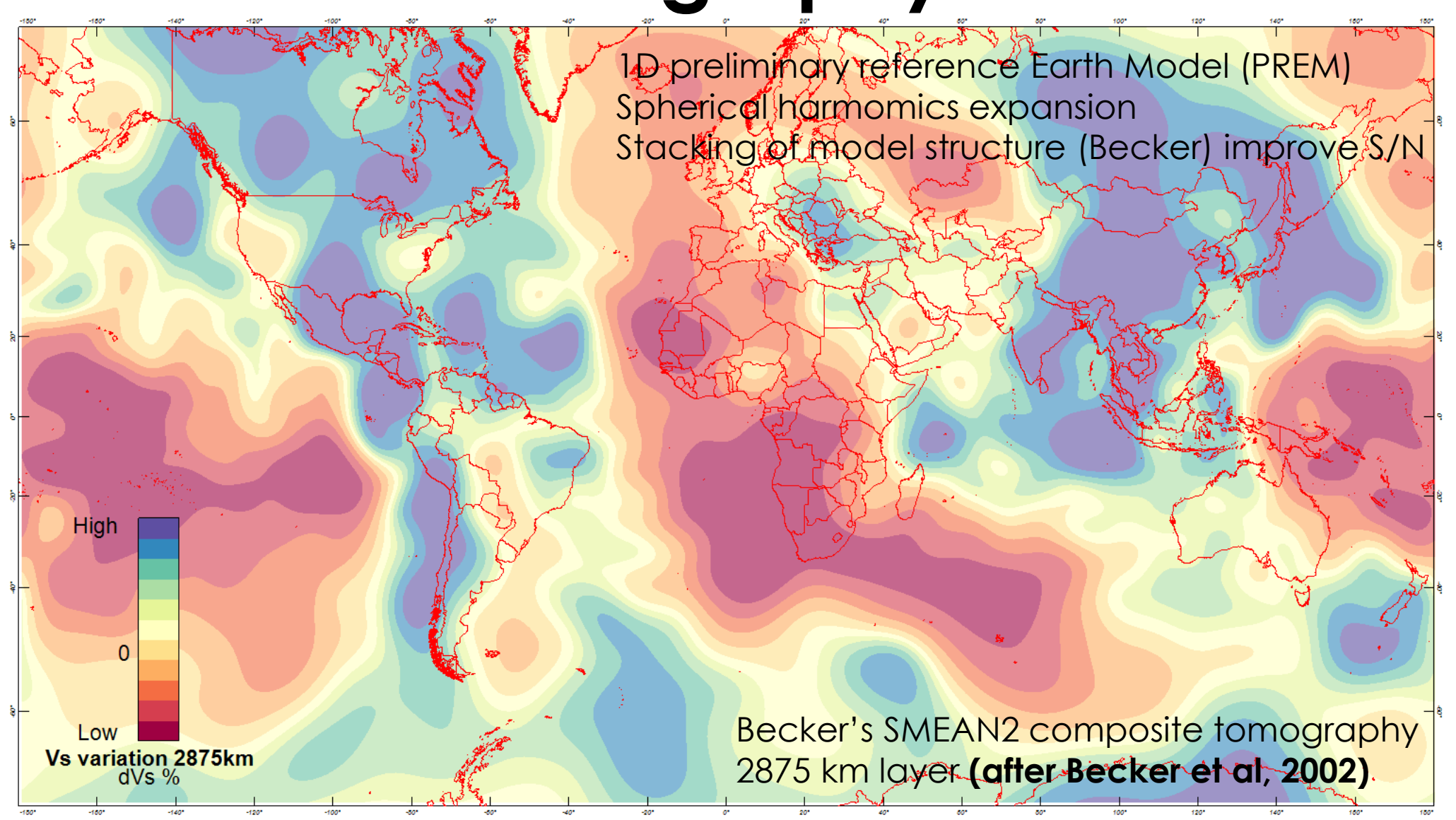
Areal coverage affects all seismic tomography models, greatest issues near surface (greater travel time coverage at core-mantle boundary)

Less ambiguity at the core-mantle boundary (S- waves do not pass through liquid outer core)





## Seismic tomography





## Handling time – the fourth dimension

#### Availability of measured data

Satellites: updated altimetry for marine coverage (Cryosat-2, Jason-1, Jason-2, AltiKa), Grace (2002-2017), GOCE 2009-2013

Bathymetry - large oceanic regions are still poorly surveyed

**Processing consequences –** understanding the construction of data sets

**Geological consequences –** refining geological mapping in areas of active deformation, understanding structural change

**Vintages of data versus resolution -** temporal variations can only be observed if the data exists, at sufficient resolution

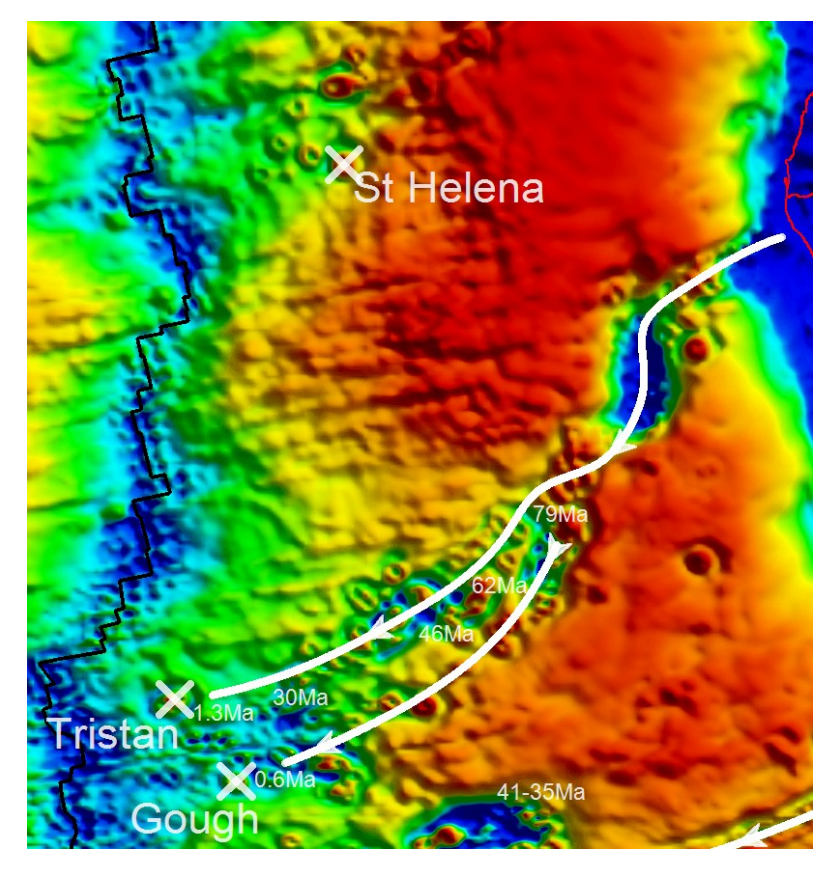
**4D Modelling –** time lapse, based on constraints, assumptions, interpolation of repeatable survey data.

#### The second way: qualitative interpretation

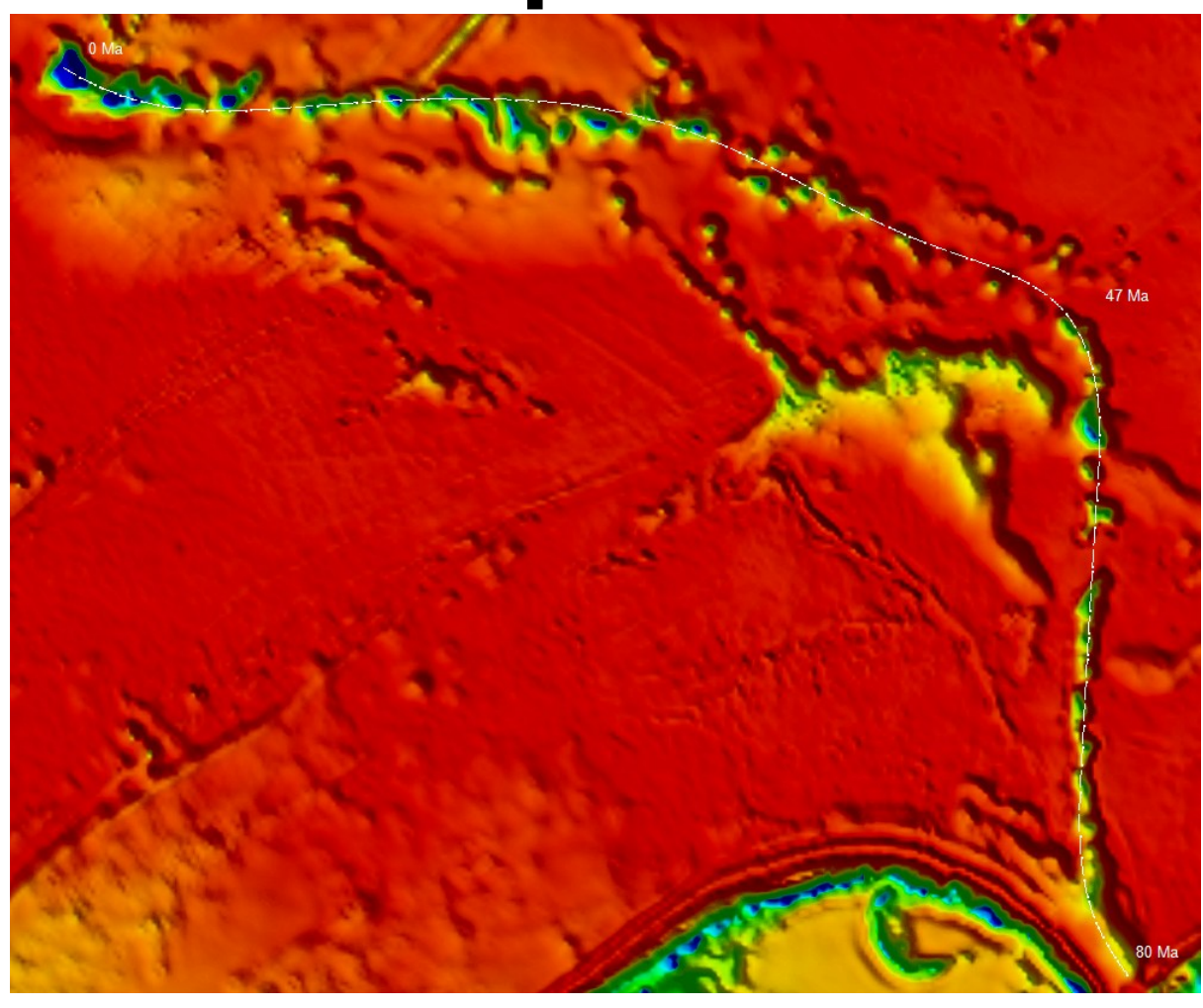


## Radiometric dating and hot spot trails

Radiometric dating enables us to estimate the latest onset of emplacement. Combined with plume trails, clearly the Earth is moving fluidly, driven by deeper structural controls.



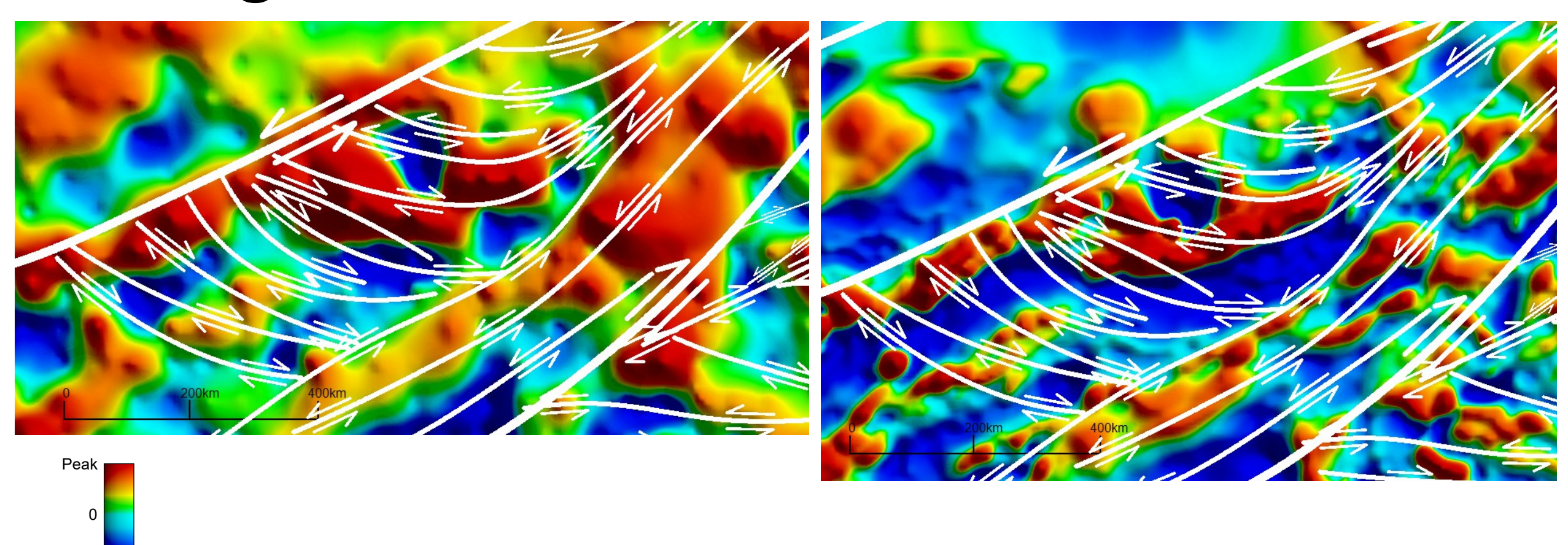
Tristan - dates from O'Connor et al, 2012



Hawaii – Emperor: dates from **Torsvik et al** , **2017** 



#### Magnetics: Namibia-Botswana border

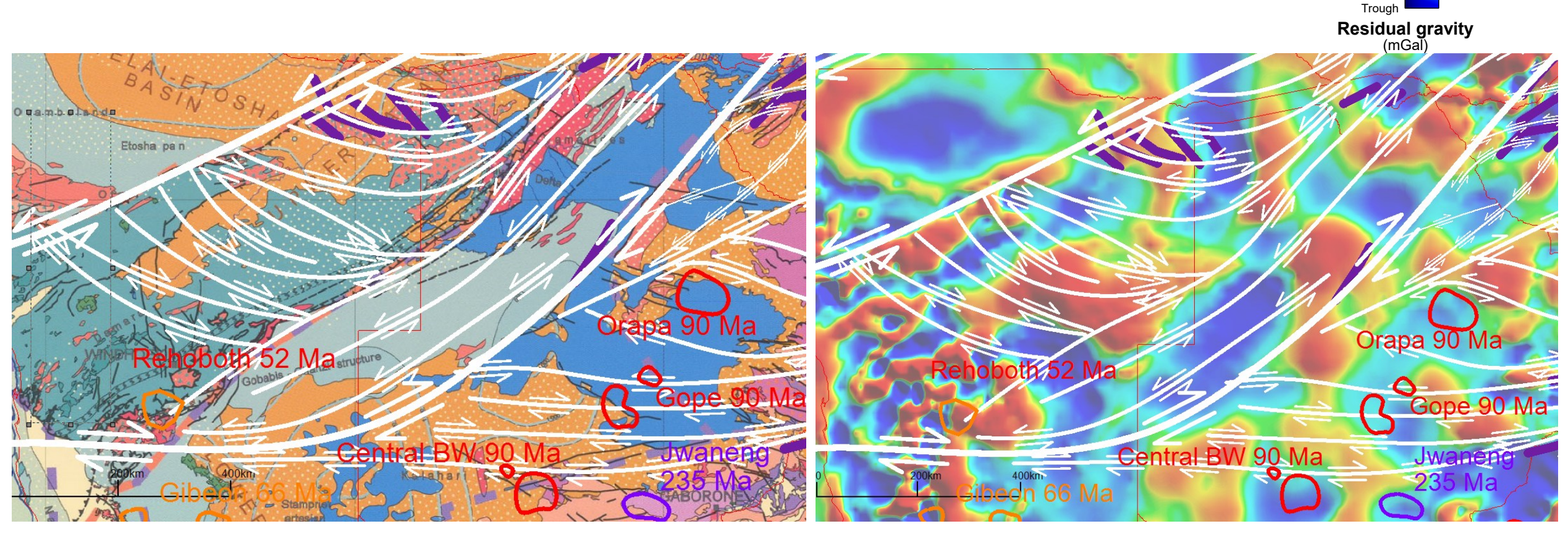


Magnetics, reduced to pole. Top left, Enhanced Magnetic Model (**Chuillat et al, 2015**), top right, World Digital Magnetic Anomaly Map, (**Quesnel et al, 2009**)

Trough

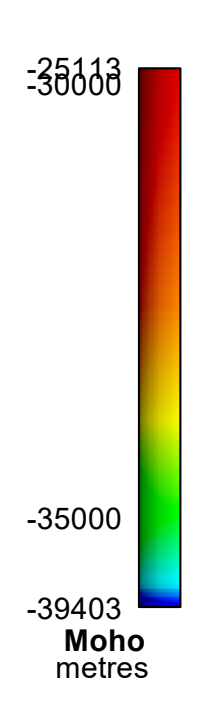
**Residual magnetics** 

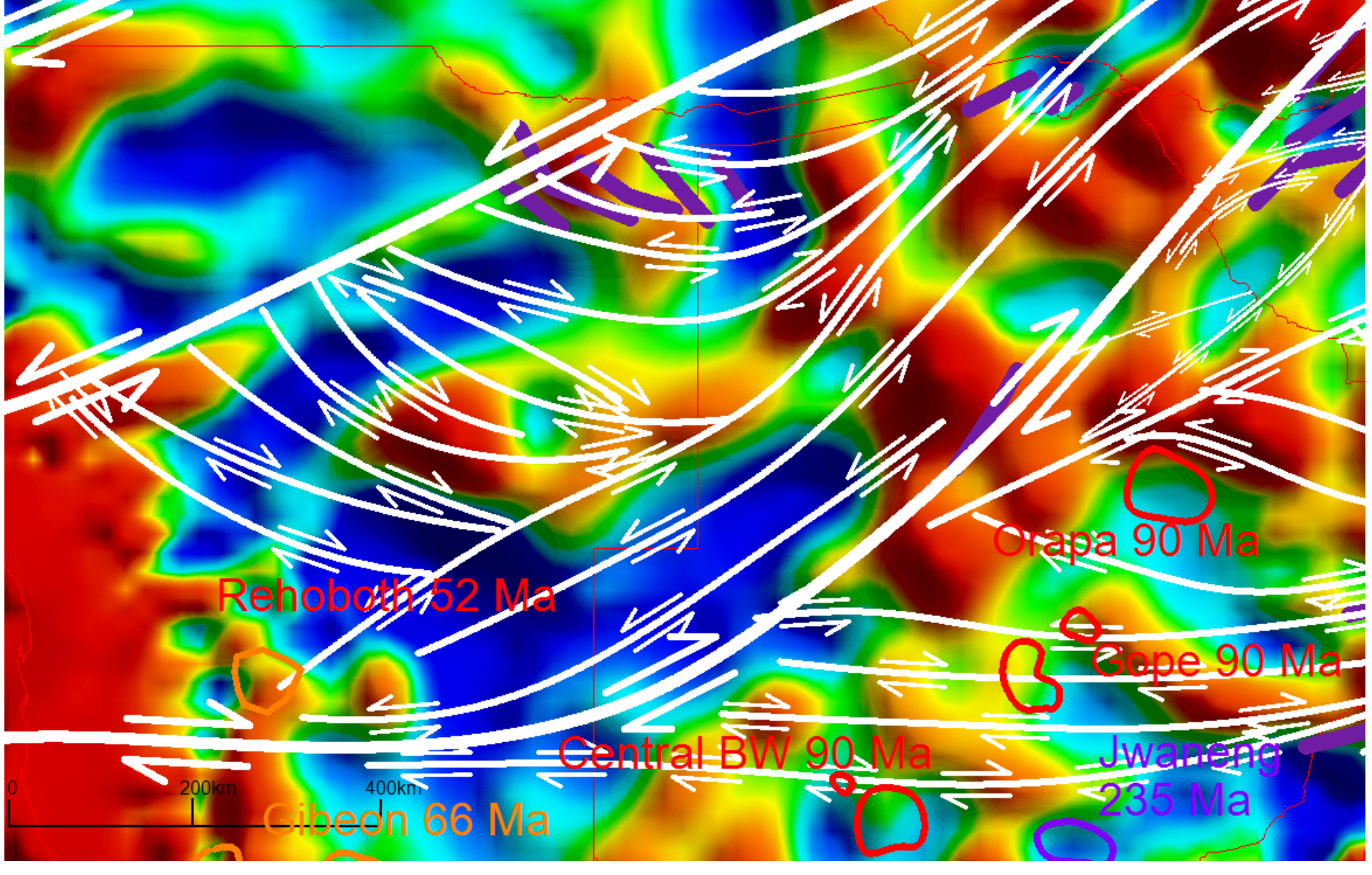
# Geology and gravity



Top left, CGWM Geology (Milesi et al, 2010), top right, shallow crustal residual gravity derived from Sandwell et al, 2014, purple faults, Permo-Triassic rifts (Macgregor, 2017), kimberlites (various sources)

#### Moho

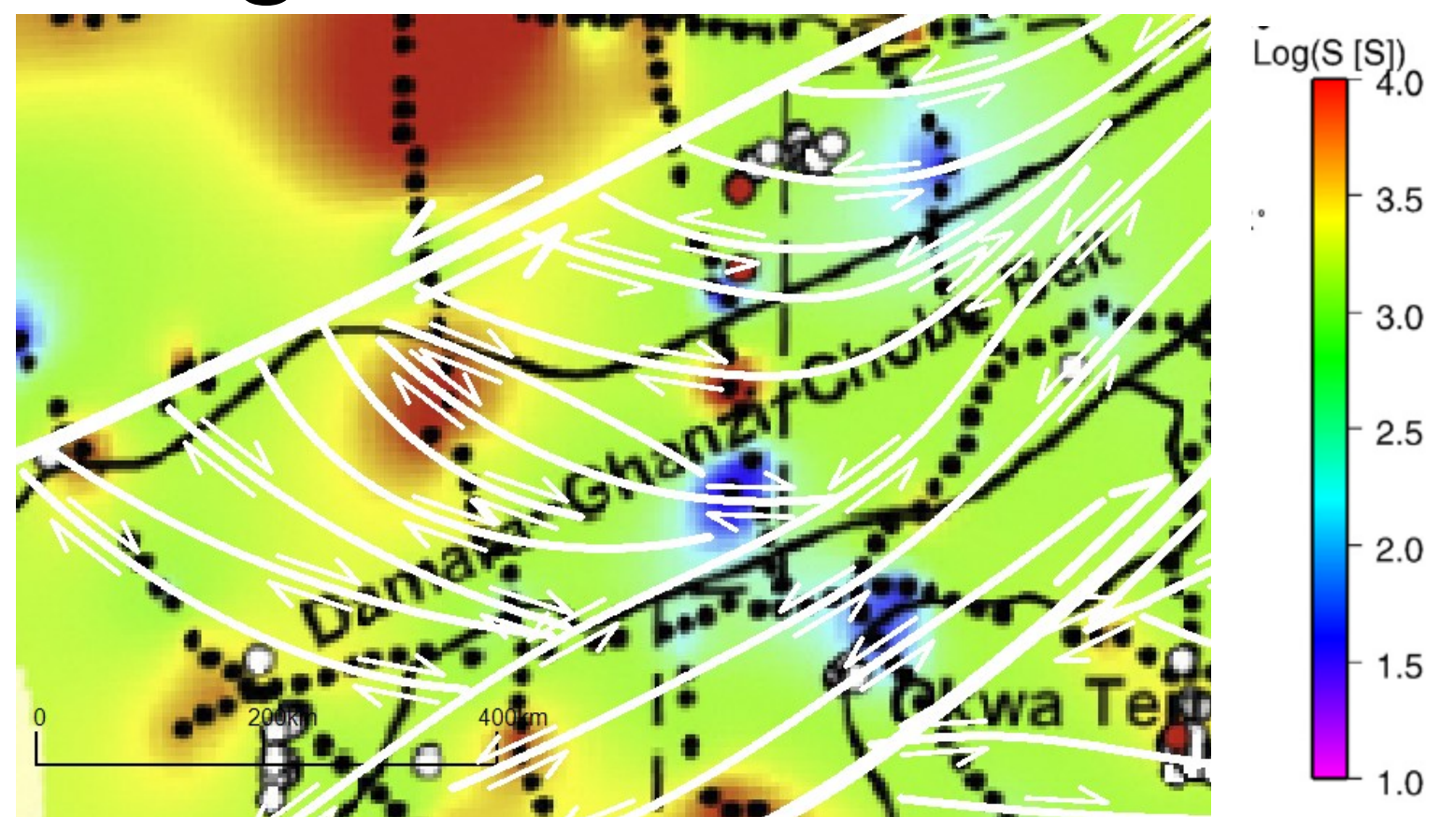




Gravity derived Moho

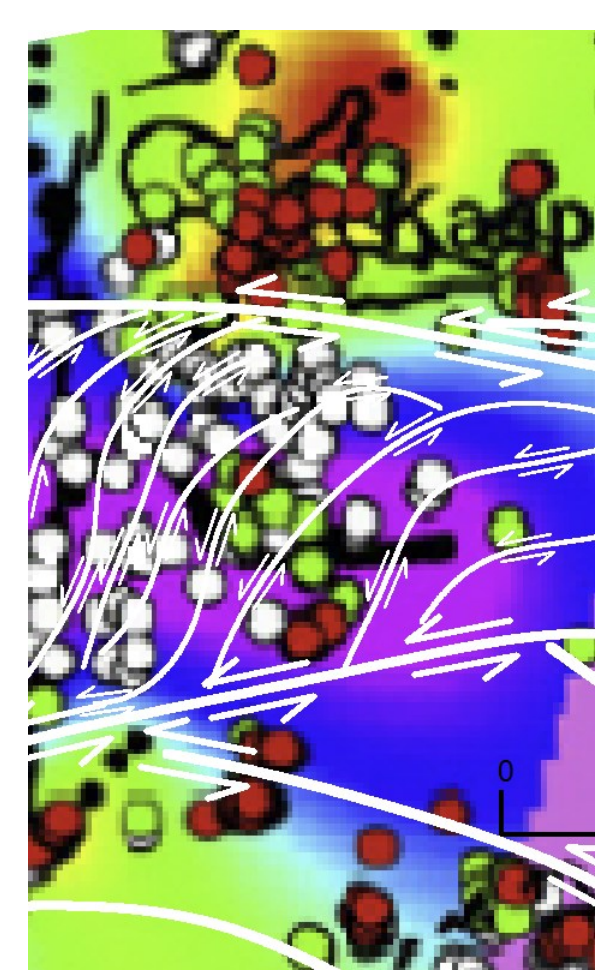


Magnetotellurics - correlations



Left: Namibia-Botswana border

Jones et al, 2009, extract from figure 6: Integrated conductivity (red – high, blue – low) distribution (40-200km - mantle lithosphere), red: diamondiferous, white: unknown, green: non diamondiferous



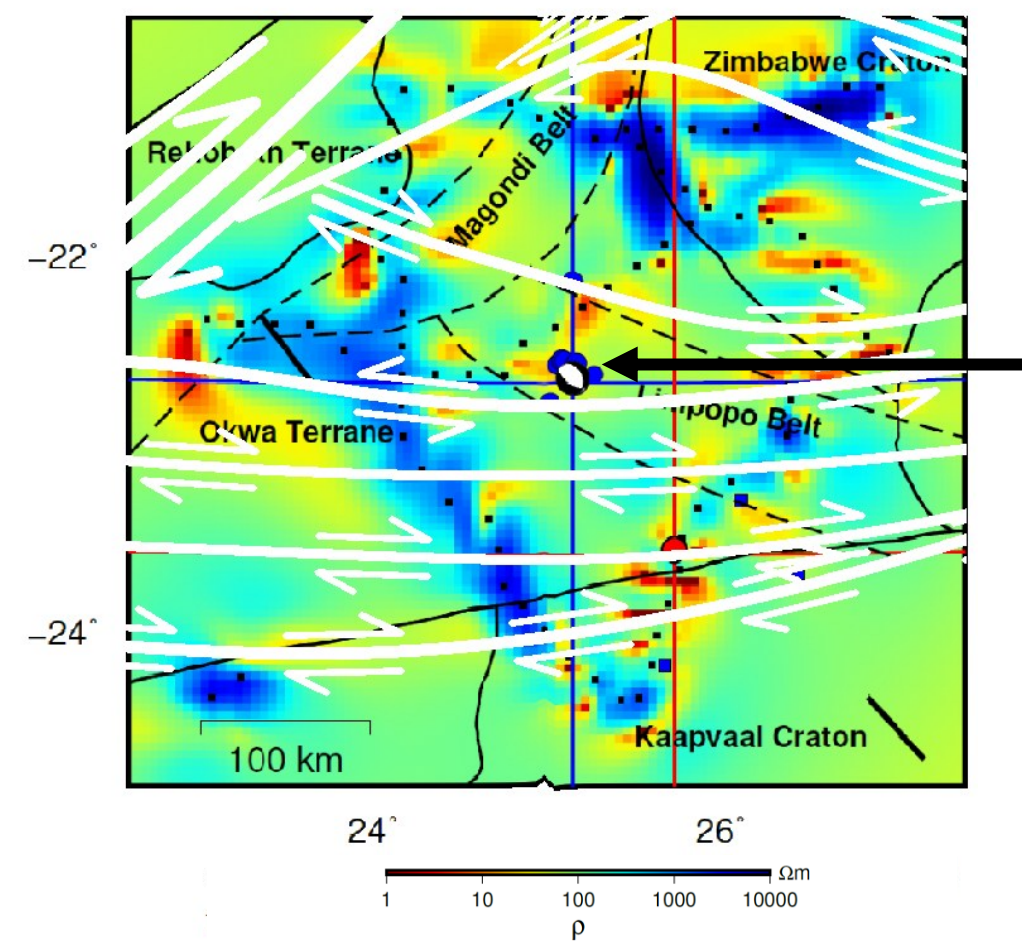
Right: margin of Kaapvaal Craton

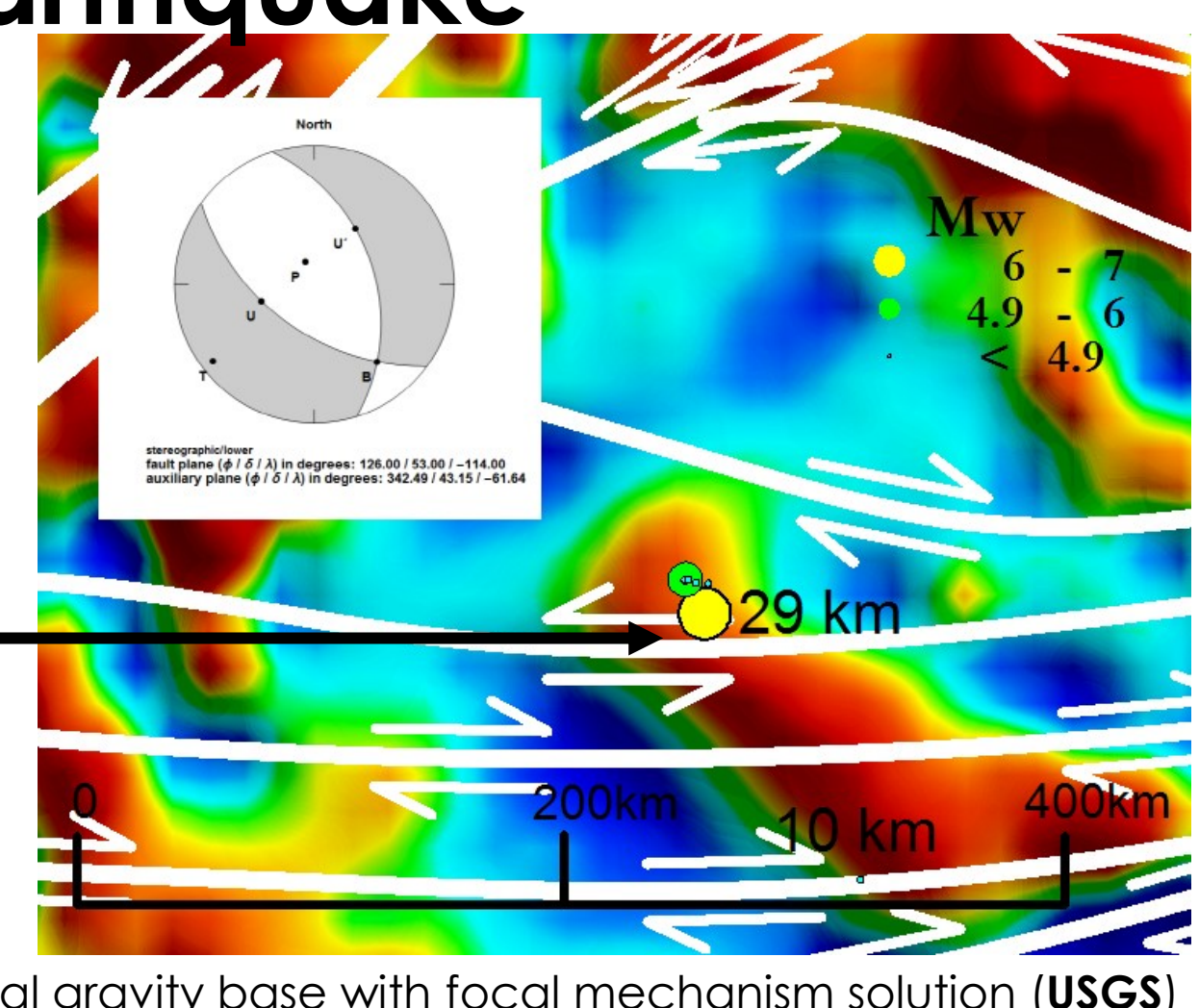




Recent Botswana earthquake

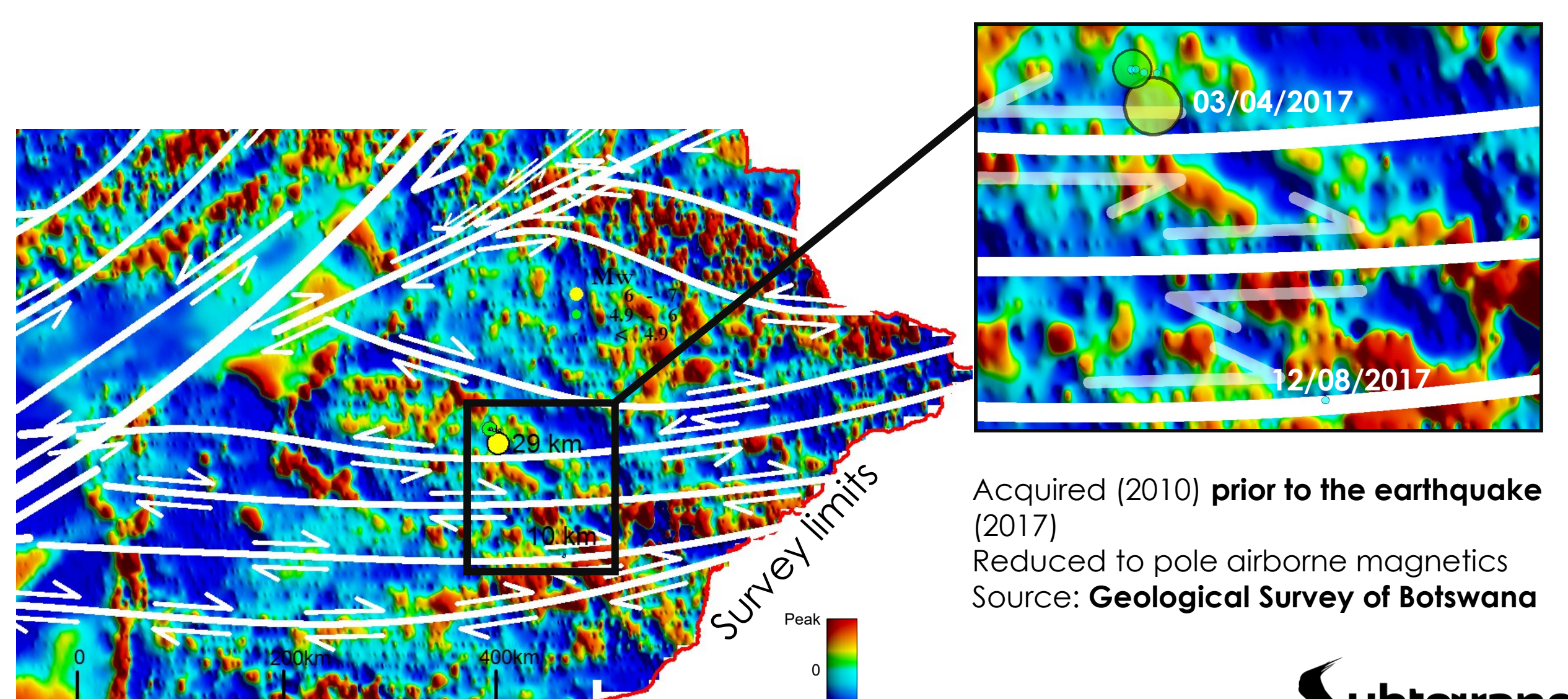
Resistivity model slice at 30km derived from 3D Samtex MT inversion (Moorkamp et al, 2019), overlain by crustal structure mapped from satellite gravity. magnetics, and other data sources





Residual gravity base with focal mechanism solution (**USGS**) for the 'unusual' 03/04/2017 **6.5 magnitude** intraplate Botswana Earthquake (synthetic normal fault), instant **brittle failure/ ductile creep.** 12/08/2017 last event (4.8 magnitude)

# Airborne magnetics



Trough

**Residual magnetics** 

# Seismicity

#### Depth (km)

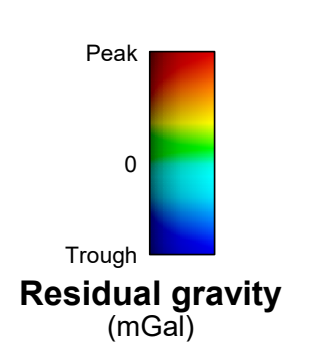
> 500 300 - 500

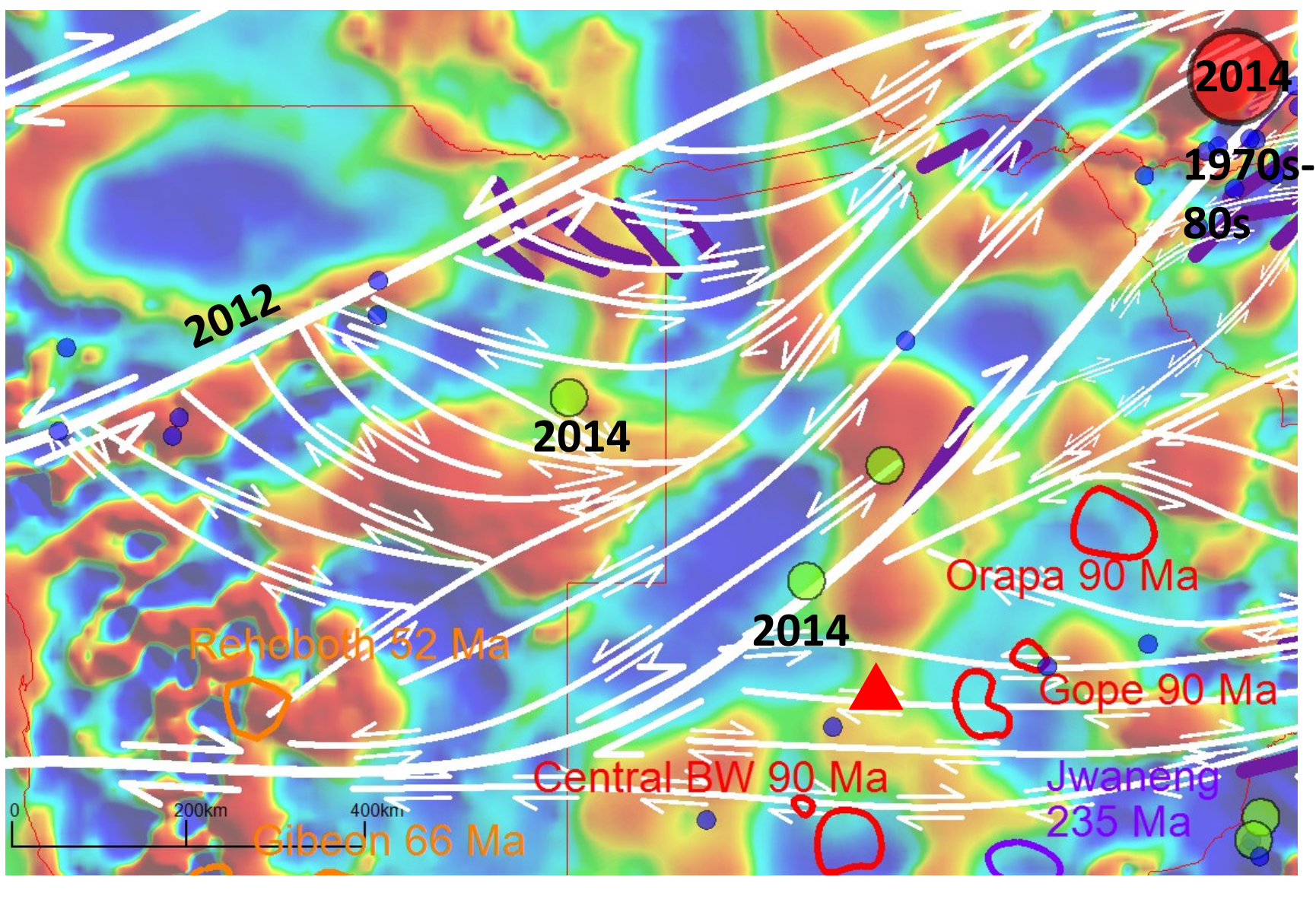
150 - 300

70 - 150

• 33 - 70

▲2017
Botswana
earthquake
(29km depth)





Shallow crustal residual gravity with 'recent' seismicity (source: IRIS data sources)





# 1999 Chi Chi ('921') earthquake

(TWO DECADES OF DESTRUCTIVE ACTIVITY)

#### **Taiwan**

Persistent strain in a region of convergent plates Western aseismic zone

7.6 magnitude earthquake, 21/09/1999

Seismic focal mechanisms constrained by

- local geology
- mapped long wavelength structure
- underlying lithospheric structure defined by seismic tomography, satellite gravity and magnetics
- -seismometers

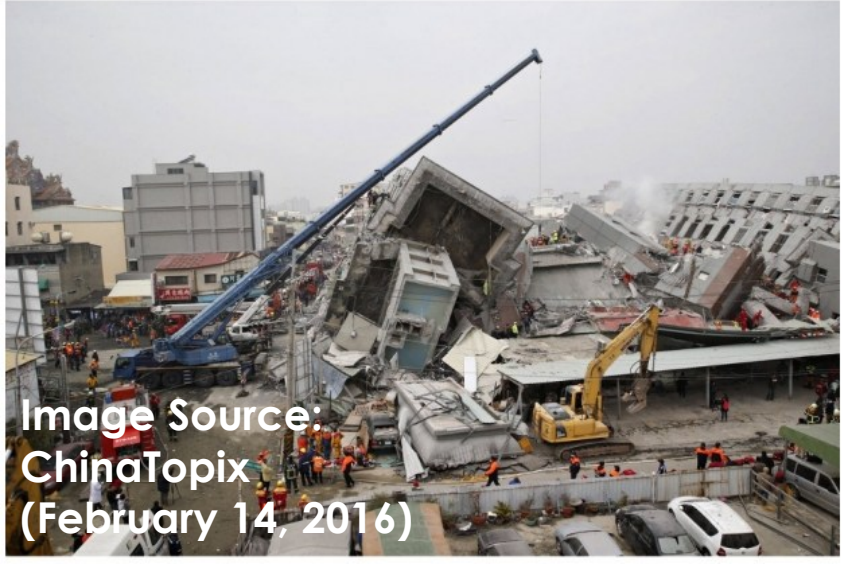
Introduction to Chi Chi using:

Sandwell et al, 2014 v27.1 (2018)

Earthquake seismicity (IRIS data sources)
Prior published research and mapped
surface faults

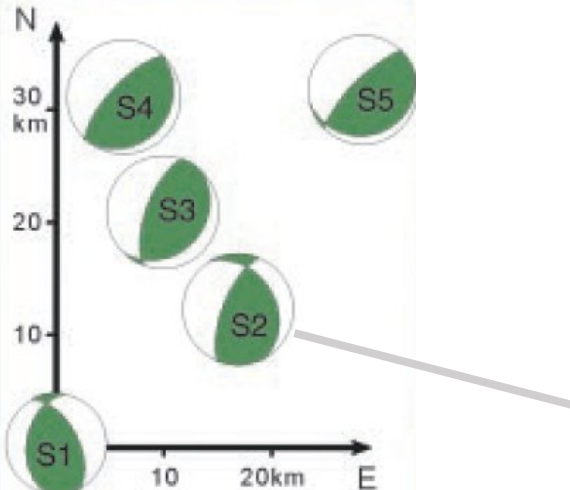




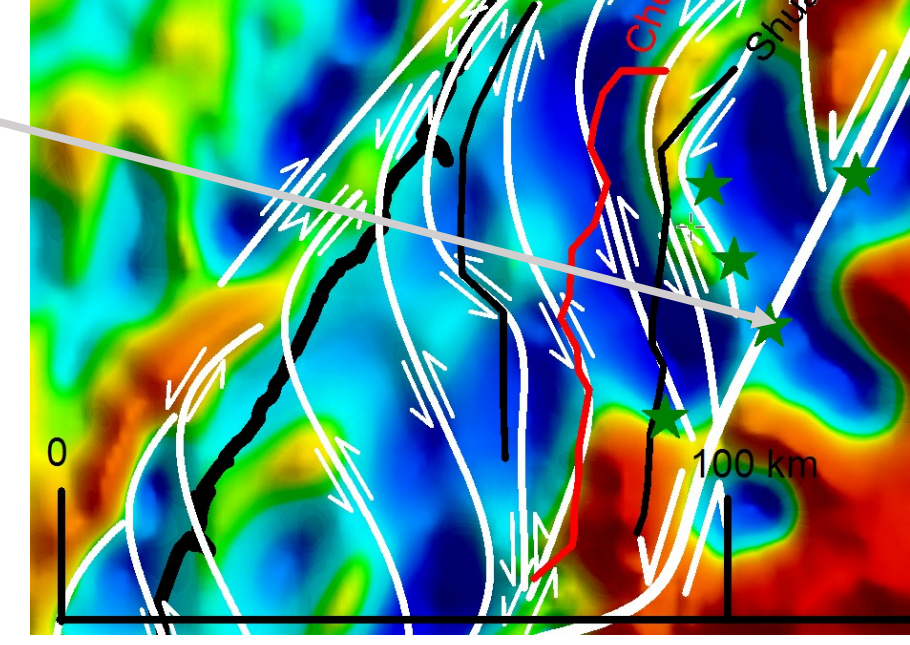


## Crustal structure at depth

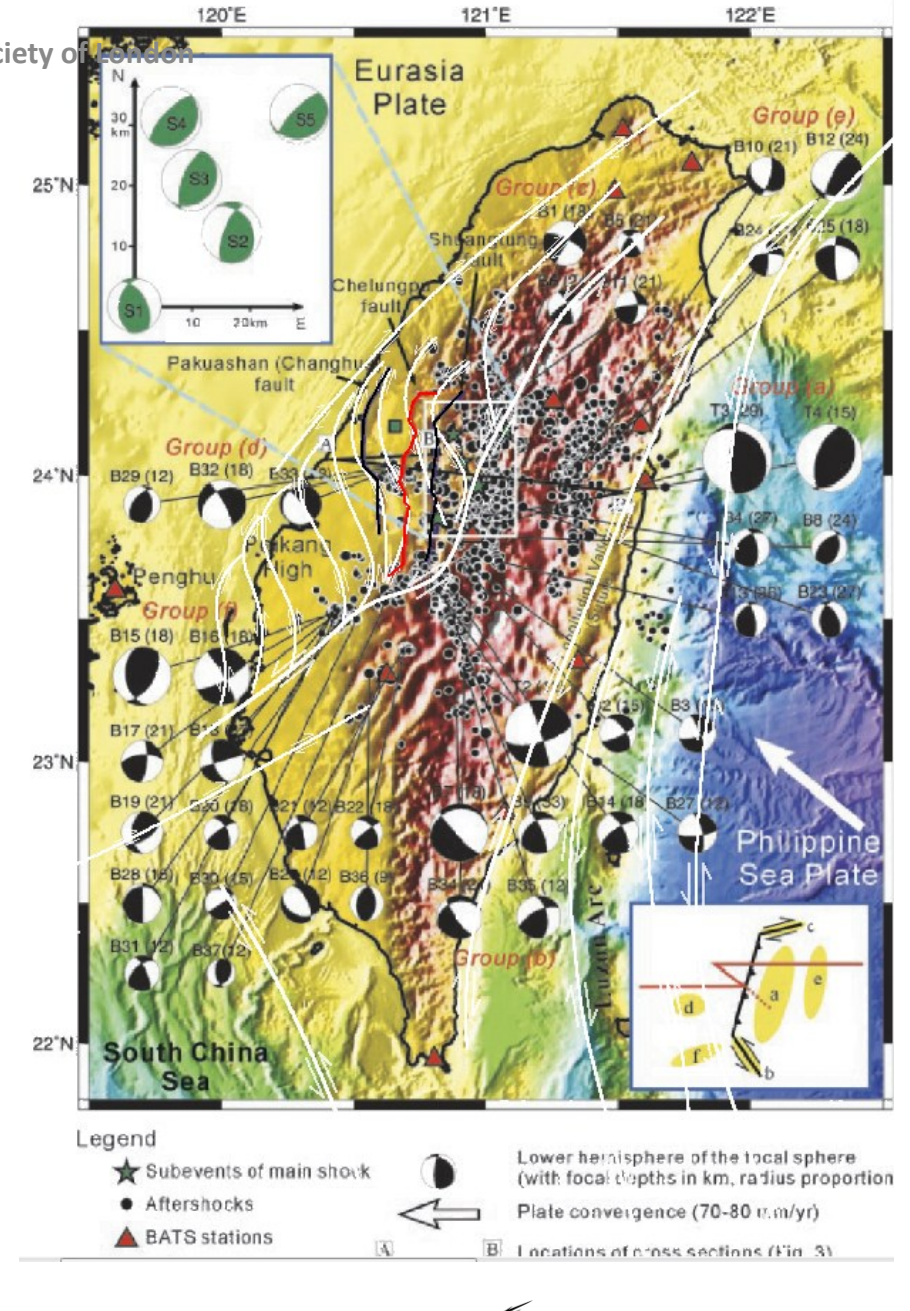
Residual gravity





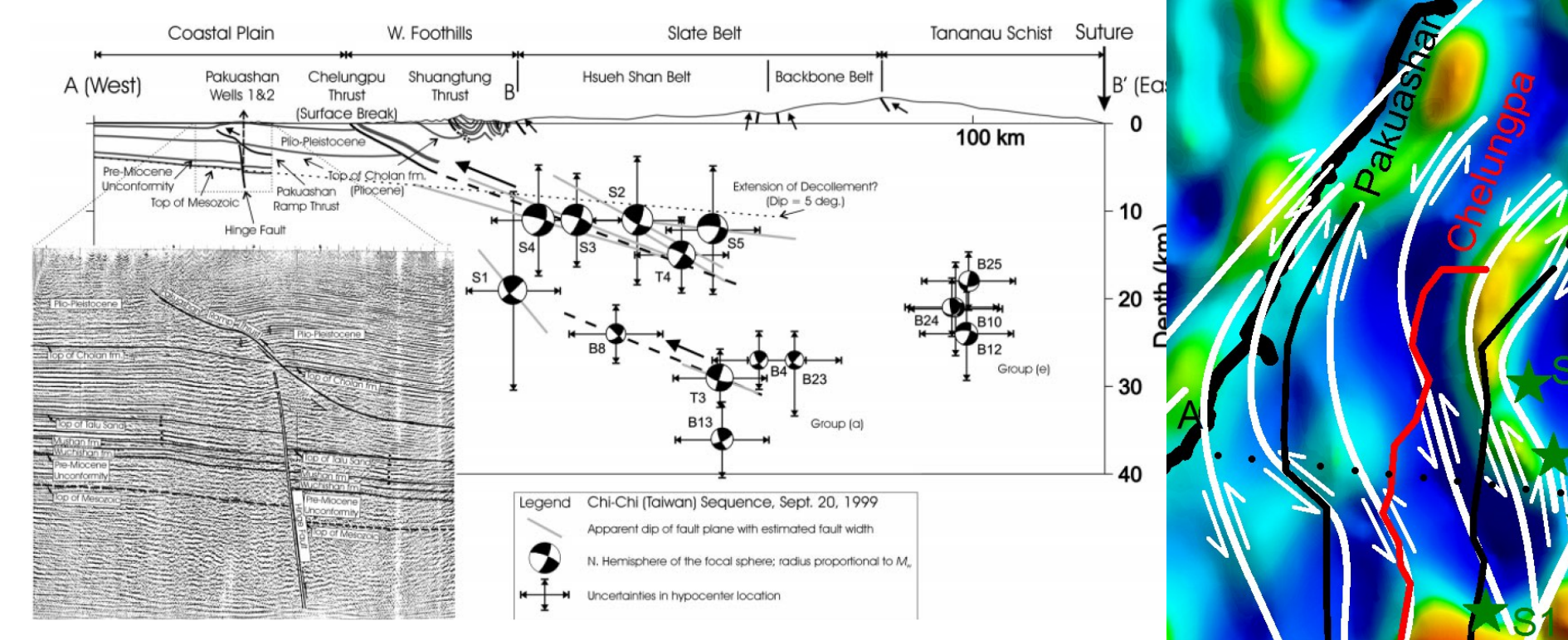


Left and right: Extracts from **Kao and Chen, 2000**. Middle: residual gravity and fault structure

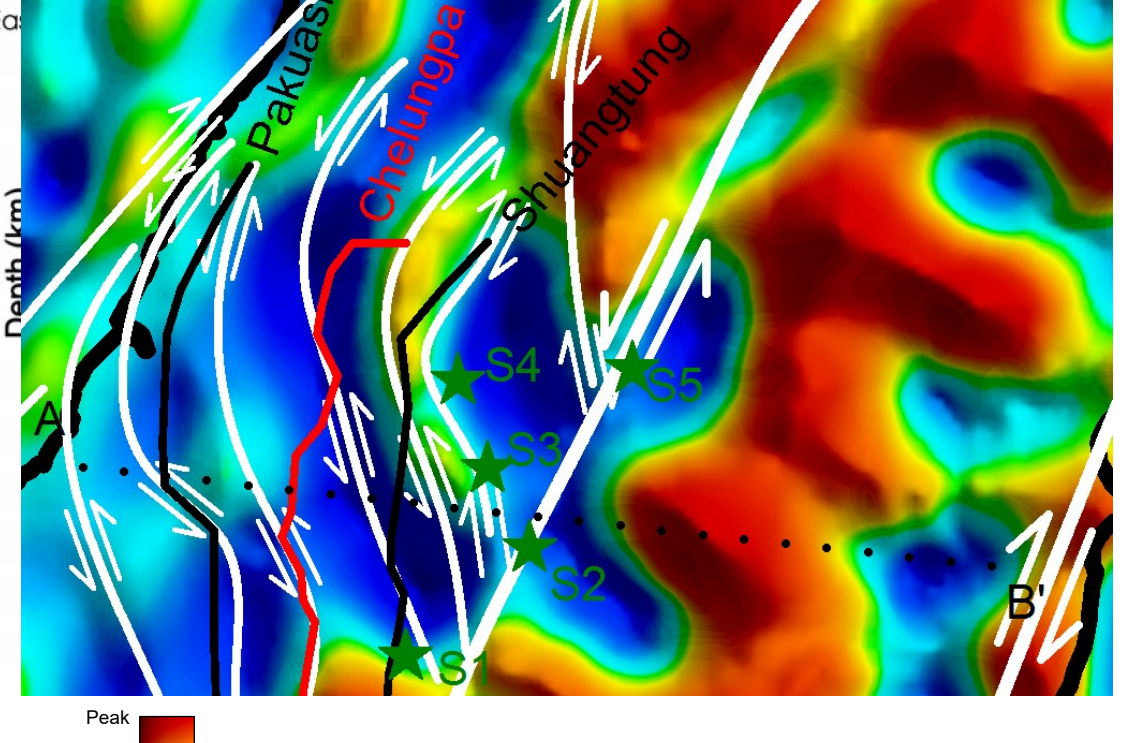


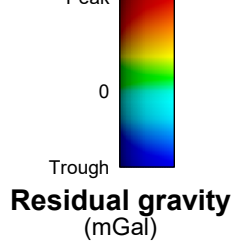


Structural configuration of Chi Chi



Extract from **Kao and Chen, 2000** 







Structural exposure - Chi Chi (Taiping)

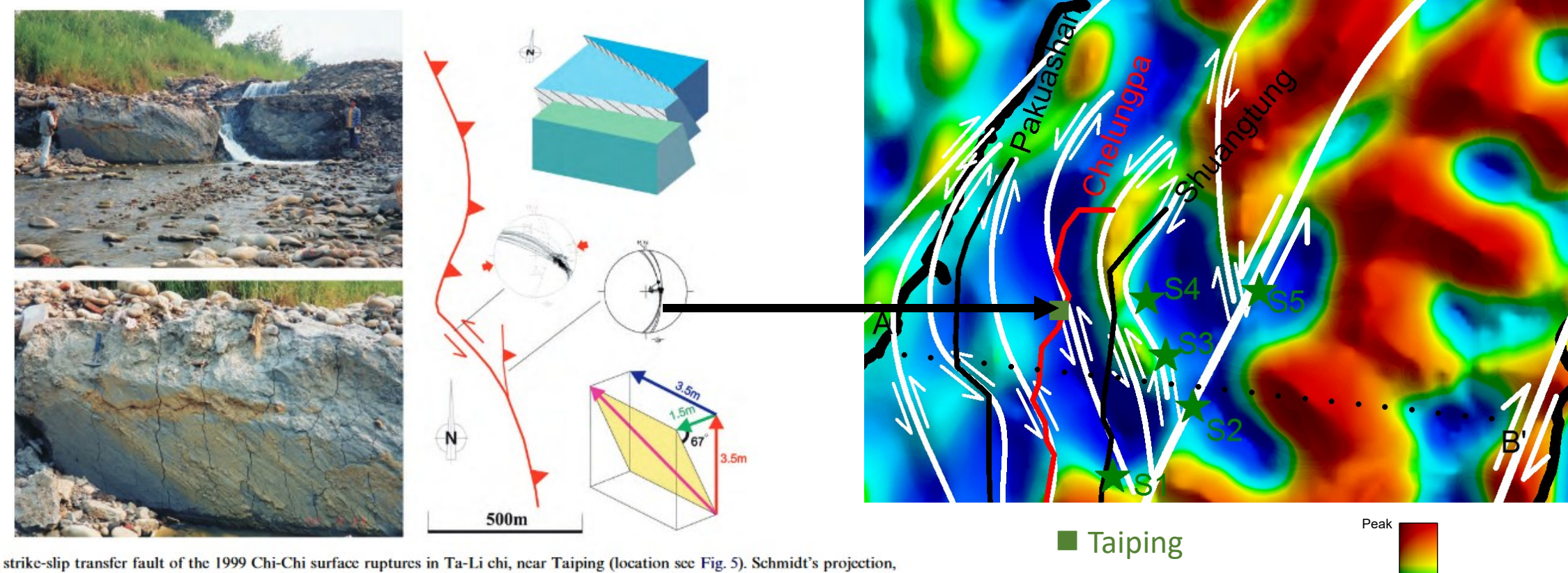


Fig. 7. Outcrop of a strike-slip transfer fault of the 1999 Chi-Chi surface ruptures in Ta-Li chi, near Taiping (location see Fig. 5). Schmidt's projection, lower hemisphere. Bedding planes shown as dashed-line great circles. Fault planes shown as thin great circles, with slickenside lineations as dots with arrows indicating the sense of motion (inward direction for reverse slip). Computed stress axes shown as stars with five branches ( $\sigma_1$ ), four branches ( $\sigma_2$ ), and three branches ( $\sigma_3$ ). Method of calculation of stress tensor: Angelier (1984). Two-fault system has been observed: the major fault (strike N125°E, dip 70° to NE) is represented by an oblique reverse fault with an important left-lateral strike-slip component, and the minor one (strike N0°E, dip 70° to E) is a reverse fault. Oblique fault striations associated with the 1999 earthquake can be clearly observed on the major fault plane.

**Subterrane**®

Trough

Residual gravity (mGal)

## The seismicity record

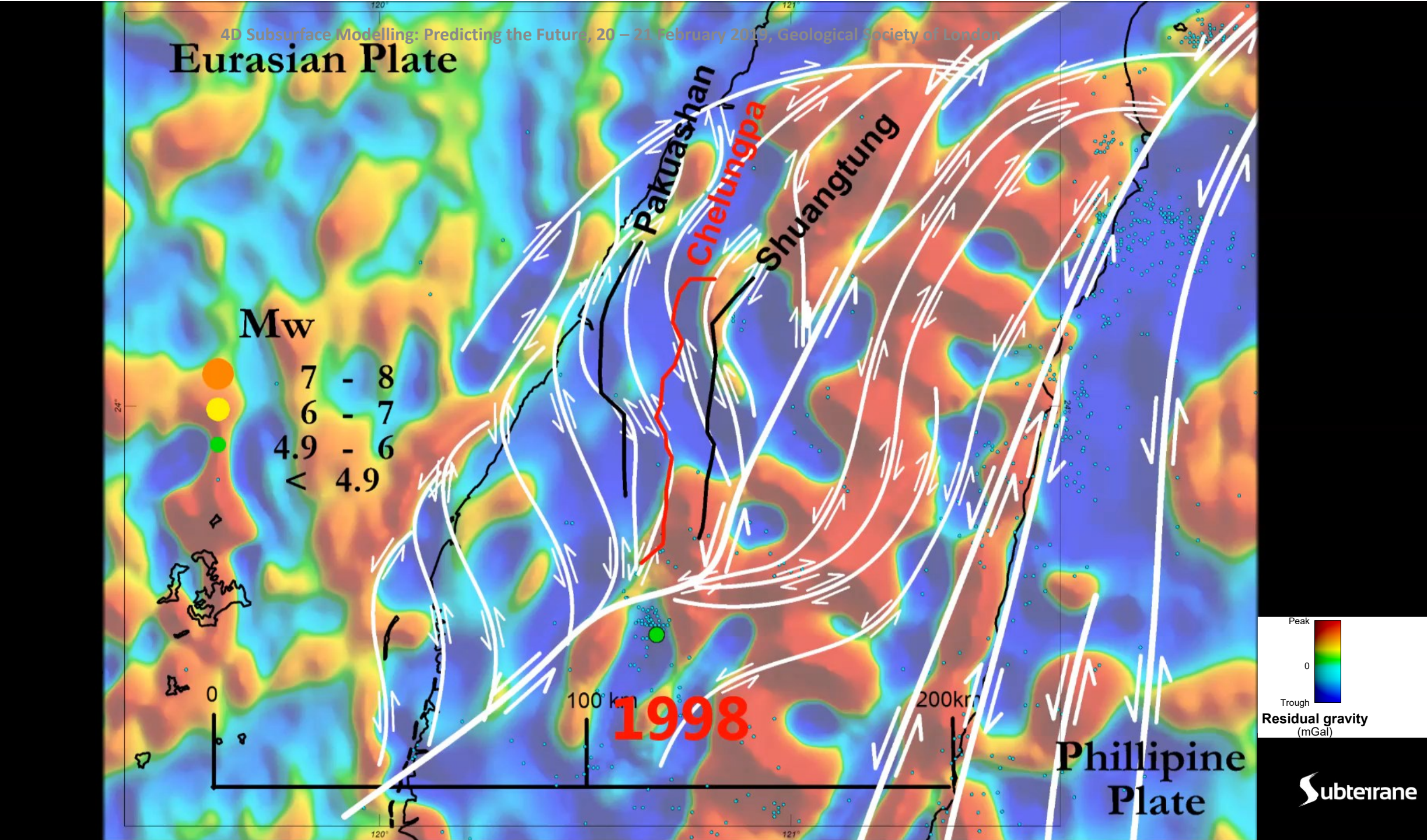
A video follows of the seismicity record (1998-2016) for shallow events (<33km), **source: IRIS data sources** 

Basemap: Sandwell et al, 2014 v27.1 (2018)

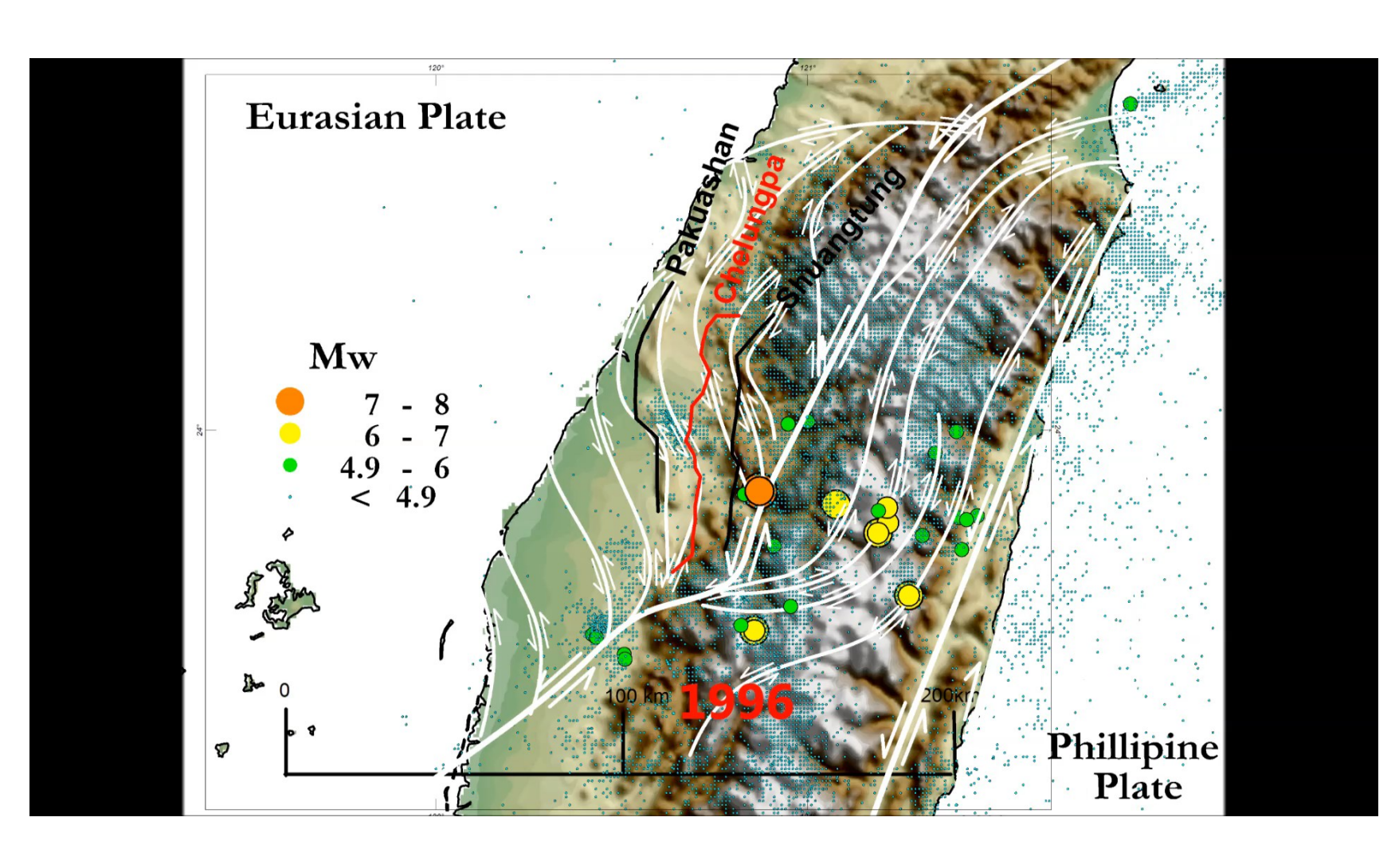
Annotated with **Kao and Chen (2000)** faults (red – active Chelungpa/black), present day crustal structure (**Subterrane (2019)** white faults)

Focal mechanism solutions published for Chi Chi and Chengkung (various)





## 1996 topography, 2000 topography



1996: **GTOPO30**, developed over a three year period through a collaborative effort led by staff at the U.S. Geological Survey's Center for Earth Resources Observation and Science (EROS).

2000: Shuttle Radar Topography Mission

Chi Chi seismicity (1999, <33 km depth to hypocentre): IRIS data sources



#### Conclusions

Qualitative interpretation is an important constraint to 4D modelling, whether time lapse or future modelling

Seismic focal solutions constrain structural interpretation, but can be ambiguous interpreted alone. A variety of important applications to infrastructure development, civil engineering, land value, ultimately hazard mitigation

Date of data acquisition is a temporal sampling issue in 4D modelling. Making satellites more cost efficient with longer missions, and enhanced measurement repeatability.

When an interpretation correlates very well with all other measurements and analysis, this provides a good basis for constrained 4D subsurface modelling of ductile geological processes



#### References

Adda et al 2017, Extensional reactivation of a deep transpressional architecture: Insights from sandbox analogue modeling applied to the Val d'Agri basin (Southern Apennines, Italy) SEG Interpretation. P SD55-66

Becker, T. W., & Boschi, L., 2002. A comparison of tomographic and geodynamic mantle models. Geochemistry, Geophysics, Geosystems, 3,1003. https://doi.org/2001.GC000168

Chulliat, A., S. Macmillan, P. Alken, C. Beggan, M. Nair, B. Hamilton, A. Woods, V. Ridley, S. Maus and A. Thomson, 2015, The US/UK World Magnetic Model for 2015-2020: Technical Report

IRIS data sources: https://ds.iris.edu/seismon/html/SM sources current.html

Jones et al, 2009, Area selection for diamonds using magnetotellurics: Examples from southern Africa Lithos 112S 83–92

Kao H. and Chen W-P, 2000 The Chi-Chi Earthquake Sequence: Active, Out-of-Sequence Thrust Faulting in Taiwan, Science, Vol. 288, p2346-2349

Kearey et al, 2009, Global tectonics, 3<sup>rd</sup> edition, published by Wiley Blackwell, pp495

Lee, J.-C. and Chan, Y.-C., 2007, Structure of the 1999 Chi-Chi earthquake rupture and interaction of thrust faults in the active fold belt of western Taiwan, Journal of Asian Earth Sciences 31 226–239

Long A.J., et al, 2011, Use of Gravity Modeling in Helping Seismic Define a Basin Prospect in Difficult Terrain: Lotikipi Plains, Kenya, EAGE Vienna conference poster

Long, A.J., Ellis, R., and Ebbing, J.(2013) Application of Iterative Re-weighting to Airborne Gravity Gradiometer Data – New Technologies to Improve Modelling Gravity Gradients

Long, A., 2019, Revolution in earthquake studies and understanding of Earth's crustal structure, white paper: https://www.terranes.co.uk/earthquake-studies.html

MacGregor, D, 2017, History of the development of Permian-Cretaceous rifts in East Africa: a series of interpreted maps through time Petroleum Geoscience, 24, 8-20

Milesi, J.P., Frizon de Lamotee, D., de Kock, G., Toteu, F., 2010, Tectonic Map of Africa at 1:10M scale CGMW ed.

Mooney et al, 1998 CRUST 5.1: A global crustal model at 5 × 5 degrees, Journal of Geophysical Research: Solid Earth, 103(B1):727-747

Moorkamp et al, 2019 Geophysical evidence for crustal and mantle weak zones controlling intra-plate seismicity- the 2017 Botswana earthquake sequence" Earth and Planetary Science Letters 506,175–183

O'Connor J. M. et al, 2012: Hotspot trails in the South Atlantic controlled by plume and plate tectonic processes, Nature Geoscience, letter, DOI: 10.1038/NGEO1583

Quesnel, Y., M. Catala'n, and T. Ishihara (2009), A new global marine magnetic anomaly data set, J. Geophys. Res., 114, B04106, doi:10.1029/2008JB006144.

Sandwell, D. T., Müller, R. D., Smith, W. H. F., Garcia, E. and Francis, R. 2014. New global marine gravity model from Cryo-Sat-2 and Jason-1 reveals buried tectonic structure. Science, Vol. 346, 6205, pp. 65-67, doi: 10.1126/science.1258213.